

6 June 2021

Towards Reliable Global Allowances for Sea Level Rise

Philip L. Woodworth ¹, John R. Hunter ², Marta Marcos ^{3,4} and Chris W. Hughes ^{5,1}

1. National Oceanography Centre, Joseph Proudman Building, 6 Brownlow Street, Liverpool L3 5DA, United Kingdom
2. Institute for Marine and Antarctic Studies, University of Tasmania, Private Bag 129, Hobart, Tasmania 7001, Australia
3. IMEDEA (UIB-CSIC), Miquel Marquès 21, 07190 Esporles, Balearic Islands, Spain
4. Department of Physics, University of the Balearic Islands, Cra. Valldemossa, km 7.5, Palma, Spain
5. Department of Earth, Ocean and Ecological Sciences, University of Liverpool, Jane Herdman Building, 4 Brownlow Street, Liverpool L69 3GP, United Kingdom

Corresponding author: P.L. Woodworth (plw@noc.ac.uk)

Abstract

Tide gauge data and information from tide, surge and ocean models have been used to calculate and validate the Gumbel scale parameters of extreme sea level distributions along the world coastline. The inclusion of ocean model information is found to result in significantly improved correspondence between observed and modelled scale parameters to that obtained using tide and surge model information alone. The scale parameters so obtained are shown to be consistent with findings reported previously, such as in assessments of the Intergovernmental Panel on Climate Change. However, the considerably improved provision of scale parameters along the coast means that coastal planners, and others concerned with impacts of sea level rise, can now undertake more complete investigations of the likely increase in sea level exceedance frequencies. In addition, coastal engineers will have access to more reliable estimates of the 'sea level allowances' needed to design defences for protecting coastal populations.

Keywords: Extreme sea level parameters; GESLA-2 tide gauge data set; Tide-surge-ocean modelling; Coastal flood protection.

1. Introduction

Numerical models of tide and surge are now being used extensively in order to compute annual maxima of sea level around the world coastline. The extreme sea level distributions obtained from these maxima at each position are usually parameterised as Gumbel distributions that are expressed in terms of two numbers: the scale and location parameters (Gumbel, 1941; Coles, 2001). The scale parameter is the important one for the present study. It sets the vertical scale of the exponential rate of reduction in the observed number of extremely high sea level events. Good estimates of scale parameters are required in order to calculate the likely increase in the frequency of occurrence of sea level extremes due to a future rise in mean sea level (the ‘multiplication factor’). A smaller scale factor implies a greater sensitivity to sea level rise. They are also needed for determining the ‘allowances’, which are the amounts by which defences need to be raised in order to provide the same likelihood of coastal flooding following a rise in sea level (Hunter, 2012; Slangen et al., 2017). The scale parameters derived from numerical models used in some previous studies are known to have been highly inaccurate and have resulted in pessimistic assessments of future flood risk (Hunter et al., 2017; Muis et al., 2017).

The Global Tide and Surge Reanalysis (GTSR) data sets of tide and surge made possible one of the first reliable attempts at estimating sea level extremes on a global scale (Muis et al., 2016), with those extreme values used to compute Gumbel scale parameters around the world coastline (archived at GTSR, 2019). The parameters were used in sensitivity studies with regard to the exposure of coastal populations to flooding due to extreme sea levels (Muis et al., 2016, 2017). However, we believe that

a software misunderstanding led to these computed scale parameters being too large.¹ When computed correctly and compared to those from tide gauge data, then it is clear that there remains a ~30% under-estimate in the scale parameters derived from tide and surge modelling at many locations, as will be demonstrated below.

The following Section 2 explains why the Gumbel distribution is a reasonable choice for parameterisation of extreme sea levels and, therefore, why Gumbel scale parameters been used in the study that follows. Section 3 then explains how Gumbel scale parameters have been determined from the GTSR and GESLA-2 data sets, and demonstrates that the two sets are far from being in agreement. Section 4 considers whether the variability in sea level due to the large-scale ocean circulation is capable of explaining at least a part of the mis-match between modelled and observed scale parameters, leading to more reliable estimates of extreme level parameters for the world coastline. We show in Section 5 that it is then possible, given a projection of future sea level rise and its uncertainty, to determine the likely increases in the frequency of sea level extremes and allowances at each point along the coast, building on the previous studies of these topics by Hunter (2012) and Hunter et al. (2013). Finally, Section 6 provides a discussion of our findings and the conclusions of the study.

2. The Gumbel Scale Parameter

We use the Gumbel scale parameter as our preferred descriptor of sea-level extremes for two main reasons. Firstly, the Gumbel distribution has been widely used by other workers and has been found to be an adequate approximation for return periods of tens to hundreds of years, which covers almost

¹ The Matlab® *evfit* function provides maximum likelihood estimates of Type 1 (Gumbel) parameters from a set of extreme minima; the software documentation (<https://uk.mathworks.com/help/stats/evfit.html>) makes clear that if one is modelling maxima then values should be entered with a reversed sign. From tests with GESLA-2 data, we have verified that the incorrect use of *evfit* leads to scale parameters about 30% too large, as we understand occurred in the earlier applications of the GTSR data sets and which we are informed has since been remedied.

all observed extremes except for the most rare events (e.g. van den Brink and Können, 2011). Secondly, our main aim was to estimate, from each sea-level record, a single parameter that would provide useful global comparisons of observed and modelled extremes. The Gumbel scale parameter is the e-folding distance in height of the Average Recurrence Interval (ARI) or Return Period or, alternatively, the slope of a plot of height against $\log(\text{ARI})$. For other distributions, such as the Generalised Extreme Value (GEV) or the Generalised Pareto (GPD) distributions, this slope may vary with ARI. However, in these cases, the derived Gumbel scale parameter represents a typical slope for the range of ARI over which the Gumbel scale parameter is fitted.

Distributions such as the GEV or GPD are generally used as a way of extrapolating the observed extremes to ARIs longer than the observational period; this is not the purpose of the present work.

For a Gumbel distribution, the scale parameter is $\sigma\sqrt{6}/\pi$, where σ is the standard deviation of the annual maxima (e.g. https://en.wikipedia.org/wiki/Gumbel_distribution; Yousef and Al-Subh, 2014). This may be used to check how close the actual extremes distribution is to a Gumbel. Using two different types of annual maxima from the GESLA-2 tide gauge data discussed below, Figures S1 and S2 in the Supplementary Information show that, in most cases, the derived scale parameters are statistically identical to those that would be obtained from a Gumbel distribution (i.e. they do not differ significantly from $\sigma\sqrt{6}/\pi$).

3. GTSR and GESLA-2 Gumbel Scale Parameters

The GTSR data set was obtained using a global barotropic model to simulate storm surges every 10 minutes for 36 years (1979-2014) at 16611 coastal points. The surges were combined with tidal elevations from the Finite Element Solution (FES) 2012 tide model (Carrère et al., 2012). Time series

of daily maximum total sea level and daily maximum surge at each coastal point are also archived at GTSR (2019).

Figure 1(a) compares scale parameters derived from the GTSR data set to those calculated from 658 tide gauge records with at least 20 years of data in the Global Extreme Sea Level Analysis Version 2 (GESLA-2) set (Hunter et al., 2017; Woodworth et al., 2017). The median length of this subset of GESLA-2 records is 39 years, similar to the length of the time series in the GTSR data set. In each case, the Matlab® function *evfit* function was used to determine the scale parameters. We have made such calculations with *evfit* before, and believe it to be reliable when used correctly. Hunter et al. (2017) describes how our *evfit* values were verified using independent software based on that of Coles (2001).

Most of the GESLA-2 records contain gaps. Therefore, in order to avoid any issues to do with the sampling of different years of data, exactly the same years were used for both GTSR and GESLA-2 with a requirement of at least 20 years in common between 1979 and 2012 (the reason for using 2012 and not 2014 will be given below). That reduced the number of useful GESLA-2 stations to 549. Because the coastal locations in the GTSR data set differed from the tide gauge positions, common locations were identified by finding the nearest GTSR coastal point. The median distance between tide gauge and nearest coastal point was 4.9 km. Figure 1(a) shows that, while the scale parameter for an individual GESLA-2 station could be said to be consistent with that from GTSR given its statistical uncertainty, most points fall below the diagonal. This means that the scale parameters from GTSR as a whole under-represent those from GESLA-2, being only 70% of the GESLA-2 values on average. There are clearly many ways of comparing such model-derived and measured quantities. The 70% in this case comes from a simple unweighted least squares fit constrained to pass through the origin using the GESLA-2 value as the independent variable (red line).

This finding means that the GTSR annual maxima are far from being accurate enough for computing the likely changes in frequency of extreme sea levels in the future. For a Gumbel distribution one can express the frequency of exceedance (N) of a level (z) as follows:

$$N = 1/R = e^{\left(\frac{\mu-z}{\lambda}\right)}$$

[1]

where R indicates the Average Recurrence Interval and λ and μ are the scale and location parameters respectively. Therefore, given a rise in sea level (H), the location parameter (μ) will increase by H and the frequency of exceedance of a given level will increase by a factor F (the 'multiplication factor'):

$$F = e^{(H/\lambda)}$$

[2]

and differentiating one has:

$$\frac{dF}{d\lambda} = -FH/\lambda^2$$

[3]

or (ignoring the sign):

$$\frac{dF}{F} = \frac{Hd\lambda}{\lambda^2} = \frac{d\lambda}{\lambda} \frac{H}{\lambda}$$

[4]

Consequently, if one takes $\frac{d\lambda}{\lambda} \sim 0.3$, which is roughly the mis-match between GTSR and GESLA-2 scale parameters in Figure 1(a), then if we assume a sea level rise of 0.5 m and a typical scale parameter of 0.1 m, one finds $\frac{dF}{F} \sim 1.5$, which is clearly inadequate for reliable impact studies.

4. Adding Ocean Variability

The importance of ocean climate variability in time series of extreme sea levels has been demonstrated in studies by Menéndez and Woodworth (2010), Marcos and Woodworth (2017) and many others. Consequently, an obvious missing component in the GTSR determination of scale parameters is that due to intra-annual, seasonal and interannual variability in the ocean circulation. This component will become particularly important where it is of comparable magnitude to storm surge variability and to the nodal and perigean cycles in extreme astronomical tides (Haigh et al., 2011).

In Muis et al. (2018), the authors extended their GTSR modelling by combining their daily maximum sea levels from tide and surge with monthly mean steric sea levels computed by the method described by Amiruddin et al. (2015). Data sets of the steric component are to be found in the same archive (GTSR, 2019). They focused on the contribution of El Niño Southern Oscillation (ENSO) variability to extreme sea levels given that ENSO is the most important ocean climate mode. The authors found significant improvements in correspondence between modelling and tide gauge measurements of extreme levels in the Pacific, but rather less so in regions with lower seasonal and/or interannual variability in sea level. However, we have found that the addition of this steric component to the present study results in only a small improvement when comparing GTSR (plus steric) scale parameters to those from GESLA-2. A similar plot to Figure 1(a) showed the steric-corrected GTSR values to be

only 74% of those from GESLA-2 on average. (One may note in passing that the Amiruddin et al. (2015) method is based on Bingham and Hughes (2012) who pointed out that its validity on continental coasts is limited to equatorial regions and low to mid-latitude eastern ocean boundaries. Elsewhere, even density-related variability cannot be expected to be captured using a simple steric sea level calculation.)

A better representation of sea level variability due to the ocean circulation would be obtained from an ocean model. As a test of this possibility, we used 5-day averaged sea surface heights for the period 1958-2012 calculated from the state-of-the-art Nucleus for European Modelling of the Ocean (NEMO) 1/12° model run (Moat et al., 2016). This is a global baroclinic model forced by wind stresses and heat/salt fluxes derived from atmospheric reanalysis fields: the Drakkar Surface Forcing dataset version 5.2 (Brodeau et al., 2010; Dussin et al., 2014). These forcings do not include surface air pressure. Therefore, these 5-day heights can be thought of as inverse-barometer (IB) corrected sea levels, and so represent steric and wind-forced dynamical ocean variability. They were linearly interpolated in time and added to the daily maximum values from GTSR, with annual maxima and Gumbel parameters recomputed at each GESLA-2 location.

Figure 1(b) shows that the scale parameters computed from GTSR+NEMO are on average 90% of those from GESLA-2, once again using the same 20 or more years in common within 1979-2012 (the limitation to 2012 mentioned above now explained). This is a satisfactorily closer agreement, although the correspondence remains slightly less than 1.0 suggesting that there could be a need for other ocean processes to be taken into account in modelling of extreme sea levels (see Discussion below).

However, a simple comparison of scale parameters is insufficient for deciding if the addition of NEMO data represents genuine improvement because scale parameters depend on the spread of annual maxima, and not whether the individual maxima are computed more accurately. Another test is to

consider the correlation between the individual GTSR+NEMO and GESLA-2 annual maxima. Figure 2(a) shows in blue a histogram of correlation coefficients between GTSR and GESLA-2 annual maxima within 1979-2012. The median coefficient of 0.513 demonstrates reasonable average correlation, the fact that they are not all 1.0 being due to inaccuracies in the modelling and/or measurements. When NEMO is also taken into account the median increases to 0.625, as shown in red.

Figure 2(b) shows a map of correlation coefficients using GTSR+NEMO while Figure 2(c) demonstrates the improvement between using GTSR+NEMO and by using GTSR alone. As might have been expected, it can be seen that the addition of NEMO has limited impact in areas such as NW Europe where annual maxima are known to be dominated by tide and surge (Merrifield et al., 2013). Most improvement is in regions such as the western Pacific islands and Japan, the western coastline of Australia and the west coast of the Americas where variability due to ENSO is important. Improvement can also be seen in the Gulf of Mexico and Mediterranean.

However, we suspect that the explanation for the improvement is more complicated than simply assigning it to interannual variability alone. Figures S3-S6 show distributions of mesoscale variability (S3), the amplitude (S4) and phase (S5) of the annual cycle (12 month harmonic of the seasonal cycle), and the interannual variability (S6), obtained from the NEMO model. These findings correspond adequately with published measurements of these quantities from satellite altimetry. Mesoscale variability can probably be disregarded as a major factor as it will not propagate to the coast without considerable dynamical modification except perhaps at ocean islands where, being stochastic, it would tend to reduce correlations. However, the modelled annual cycle can be seen to be as large as interannual variability, especially in the northern hemisphere, even though the model does not include seasonal processes due to changes in ocean mass. It is possible, therefore, that some of the improvement might come from a better representation of the seasonal cycle in the extremes, and not only from ENSO-type interannual variability. One notes that while the addition of NEMO benefitted

the western Pacific islands, some of those in the central and eastern parts of the basin remain for further improvement.

One concern in combining NEMO with GTSR information in this way is that, because both models are wind-driven, there could be a contribution to the computed extremes due to double counting of wind-driven storm surges on 5-day timescales. The ideal approach to this problem would be to remove 5-day mean surge values from GTSR before combining with NEMO. However, this option was not available to us as we did not have access to the original GTSR 10-minute time series, but only to the daily maxima described above. Therefore, in order to assess how large a problem this was, we made use of the 0.25° resolution Advanced Global Barotropic Ocean Model (AGBOM, Stepanov and Hughes, 2004; Hughes et al., 2018) to provide daily IB-corrected sea levels for 1990-2003, with daily values averaged into 5-day means. Such values will thereby represent the wind-driven component of sea level variability on 5-day timescales. Standard deviations of this variability were computed for each of the 16611 GTSR locations and are shown in Figure S7a. These values are similar to those for the full ocean shown in Figure 5 (top) of Hughes et al. (2018) and have a median value of 2.1 cm. Using longer 35-day means, the median standard deviation reduced to 0.96 cm, although sections of coast such as the eastern North Sea, Baltic, Gulf of Carpentaria, Gulf of Thailand, Yellow Sea, Bering Strait and Arctic Russia indicated values of ~5 cm or more (Figure S7b).

Therefore, as a sensitivity test, we repeated the above calculations for GTSR+NEMO extreme sea level values and scale parameters using interpolated 35-day NEMO means instead of 5-day means, thereby reducing any double-counted storm surge contribution as far as possible, at the expense of losing skill in NEMO on timescales of less than a month. Almost identical results were obtained, with a distribution of correlation coefficients shown in green in Figure 2(a), a median correlation coefficient of 0.614, and virtually the same spatial distributions as in Figure 2(b,c). Therefore, for the remaining discussion of this paper we have focused on the use of the original 5-day NEMO mean values, given

that they provided a marginally higher median correlation, and that findings below are unaffected by the choice of using either 5-day or 35-day smoothed NEMO levels.

Recently, the group responsible for the GTSR models has published a new global tide+surge data set with improvements to both tide and surge modelling, including an increase in spatial resolution along the coast from 5 to 2.5 km. This data set is called CoDEC-ERA5 (Coastal Dataset for the Evaluation of Climate Impact using the ERA5 climate reanalysis data set of the European Centre for Medium-Range Weather Forecasts, Muis et al., 2020) and provides measurements at 14110 coastal points covering the period 1979-2017. The authors have to date made available the Gumbel scale parameters computed from this data set, but not the tide and surge time series from which they were calculated. Therefore, it is not possible as yet to use the above methods to investigate how well the addition of NEMO would benefit the new modelling.

However, there are various ways to decide whether CoDEC-ERA5 might lead to more accurate Gumbel parameters. One way is to make a simple comparison of scale parameters derived from all GTSR or CoDEC-ERA5 information (1979-2014 and 1979-2017 respectively), to those obtained from all GESLA-2 records with at least 20 years of data i.e. without the restriction of 1979-onwards (Figures 3a,b respectively). Because of differences between the GTSR and CoDEC-ERA5 grids, a coarse 50 km maximum distance requirement was imposed between a GESLA-2 location and each of the nearest model grid points; given that the median distances are ~5 km in each case, few GESLA-2 data points are rejected by this selection.

Figure 3(a) is little different from Figure 1(a), indicating once again that GTSR scale parameters underestimate GESLA-2 ones. In this case, GTSR values are approximately 72% of GESLA-2 ones on average, an almost identical value to that obtained previously using matching years in the calculations. Similarly, Figure 3(b) demonstrates that, even though the CoDEC-ERA5 modelling might have

improved on GTSR, its scale parameters remain lower than GESLA-2 ones (73%). However, the scatter of points using CoDEC-ERA5 is somewhat reduced. The differences between GTSR scale parameters in Figure 3(a) and those suggested by the fitted slope times the GESLA-2 scale parameter have an approximately normal distribution, with the difference between 90 and 10 percentiles (essentially full-width) of 0.084 m. The corresponding difference in percentiles for CoDEC-ERA5 in Figure 3(b) is 0.066 m, supporting a genuine improvement in tide+surge modelling. In particular, there are fewer instances of the model producing much larger scale factors than those derived from GESLA-2.

Another way to test CoDEC-ERA5 is to estimate the scale parameters that might be obtained using CoDEC-ERA5 modelling in combination with NEMO (λ_{CN}), instead of GTSR in combination with NEMO (λ_{GN}), by assuming that Gumbel scale parameters from each component can be combined quadratically. This assumption was tested using information for 1979-2012 at every GTSR location and by calculating scale parameters that would be inferred for GTSR+NEMO using GTSR and NEMO annual maxima alone i.e.

$$\lambda^2_{CAL} = \lambda^2_G + \lambda^2_N \tag{5}$$

where subscripts indicate GTSR alone (G), NEMO alone (N) and calculated (CAL). The latter can then be compared to those computed from GTSR+NEMO annual maxima (λ_{GN}) as shown in Figure 4(a). Satisfactory agreement can be seen, although many calculated values lie below the diagonal for λ_{GN} values larger than about 0.15 m. These coastal locations correspond closely to those identified above from AGBOM modelling as having higher standard deviation of wind-driven variability on 5-day timescales (Figure S7a). In turn, this implies that some double counting must be occurring in these areas and that Equation 5 cannot be expected to hold. (One may note that, if there was 100% double counting, i.e. GTSR and NEMO were modelling identical processes, then the scale parameters for GTSR

and NEMO would be identical, and the λ_{CAL} values in Figure 4(a) would have been 1/√2 of the corresponding λ_{GN} values on average, instead of being approximately the same).

We can persevere with this approach given that there are relatively few GESLA-2 stations in the areas identified above as probably suffering from double counting. Therefore, we have estimated values of λ_{CN} using:

$$\lambda_{\text{CN}}^2 = \lambda_{\text{C}}^2 + \lambda_{\text{N}}^2$$

[6]

where subscripts indicate CoDEC-ERA5 + NEMO (CN), CoDEC-ERA5 alone (C) and NEMO alone (N). Ideally, all parameters in such combinations should be obtained from exactly the same years, as was the case for the test of Equation 5. However, that is not possible for Equation 6, for the reasons given above. As the object of the exercise is to compare the λ_{CN} to the scale parameters from GESLA-2, we computed λ_{N} for exactly the same years as we had GESLA-2 information within 1979-2012 (minimum of 20 years), but were obliged to use the λ_{C} values calculated for 1979-2017 by Muis et al. (2020). The comparison of λ_{CN}^2 to GESLA-2 is shown in Figure 4(b). The modelled scale parameters (CN) are 85% of the GESLA-2 ones on average, with a 10-90 percentile width of their differences of 0.054 m. The fact that this is a somewhat tighter distribution than GTSR+NEMO in Figure 1b (in which scale parameters are 90% of the GESLA-2 ones on average but with 10-90 percentile width of 0.090 m) is another encouraging result, and suggests that even more accurate calculations of the allowances discussed in the next section might be possible, once we are able to combine CoDEC-ERA5 with an ocean model such as NEMO more rigorously. Of course, the accuracy of any comparisons to GESLA-2 such as those above will always be limited by whatever inaccuracies there are in the historical tide gauge data.

5. Changes in Frequency and Allowances

We can now move to the objectives of the present study, to calculate the likely increase in the frequency of occurrence of extreme sea levels due to a future rise in mean sea level and to determine the allowances required for coastal protection.

Figure 5(a) shows the reciprocal of scale parameters calculated from GESLA-2 at each location. This is essentially the same figure as Figure 3(b) of Hunter et al. (2017), although the scale parameters in the latter were computed using the alternative Coles (2001) software. An exponential of the product of sea level rise and the reciprocal of the scale parameter determines the increase in the frequency of extreme sea levels using a Gumbel distribution (Equation 2). Figure 5(b) shows the corresponding reciprocals of scale parameters derived from GTSR+NEMO, suggesting that, at first sight at least, the modelled reciprocals are similar to those of GESLA-2 around the world coastline, the Mediterranean appearing to be one exception. An almost identical global coastline distribution is obtained using GTSR+NEMO 35-day smoothed scale parameters.

To calculate the likely increase in frequency (the ‘multiplication factor’, F), we first assume a uniform sea level rise of 0.5 m and apply Equation 2, resulting in Figure 6(a) which has many similarities to Figure 13.25(a) in the Intergovernmental Panel on Climate Change Fifth Assessment Report (IPCC AR5) (Church et al., 2013). The AR5 figure included information only at GESLA-2 locations without the now considerably improved coverage of the global coastline provided by the modelling.

Figure 6(b) shows the multiplication factor using the spatially-dependent RCP4.5 scenario for regional sea level rise between the epochs 1986-2005 and 2081-2100 (Figure 13.19a of Church et al., 2013; ICDC, 2020). That scenario has a global mean of 0.48 m and includes contributions from vertical land movements caused by Glacial Isostatic Adjustment (GIA) and response to ongoing changes in land ice.²

² A slightly updated version (Version 5, 27-March-2014) of the data presented in the AR5, and used in this study, is available from ftp-icdc.cen.uni-hamburg.de/ar5_sea_level_rise.

One notes that Figure 6(b) is similar to Figure 6(a), apart from at high northern latitudes where SLR is negative due to GIA and response to ongoing changes in land ice. This becomes more understandable from inspection of Figure S8 which shows the same values for SLR as Figure 13.19a of Church et al. (2013) but for the coastline only.

The RCP4.5 projection of sea level rise is accompanied by a spatially-dependent estimate of the model uncertainty, which has an average standard deviation of 0.15 m but with much larger values at high northern latitudes (Figure S9).³ The AR5 considered that this model uncertainty might be only about 58% of the actual uncertainty, although the evidence for this is not strong. We here use the model uncertainty as our estimate of standard deviation; we may, therefore, be underestimating the true allowance (see discussion of this topic in McInnes et al., 2015). The availability of uncertainty estimates enables the computation of coastal protection ‘allowances’, which are the amounts by which defences need to be raised in order to provide the same likelihood of coastal flooding following a rise in sea level. We follow the approach of Hunter (2012) for this calculation although variations on the method are possible (e.g. Buchanan et al., 2016). Assuming the uncertainty is normally-distributed, then the allowance (A) can be calculated as:

$$A = SLR + \frac{\sigma^2}{(2\lambda)}$$

[7]

where SLR is the spatially-dependent sea level rise in RCP4.5 and σ is the corresponding standard deviation of the uncertainty. Once again, one notes the dependence on the reciprocal of the scale parameter.

³ The large uncertainty at high northern latitudes is mainly due to significant disagreement between the two GIA models employed in the sea level projection.

Figure 7(a) shows how allowances (A) vary around the world coastline in RCP4.5, while Figure 7(b) focusses only on the second term in Equation 7, which is the main aspect of interest for the present study. It can be seen that this second term contributes one or two decimetres to the allowances, apart from certain local areas such as the northeast coast of North America where it is several decimetres and, therefore, comparable in magnitude to the first term (SLR). Allowances for that particular area have been studied in detail by Zhai et al. (2015). The second term is also larger than two decimetres at central Indian Ocean islands, the east coast of Madagascar and in the Caribbean. Figure 7(c) presents the ratio $\left[\sigma^2 / (2\lambda)\right] / A$ which has a median value of 0.18 for the world coastline but larger values in the aforementioned areas. There are high latitude locations where the overall allowance (Figure 7(a)) and the ratio (Figure 7(c)) are negative due to the contribution to SLR of GIA and response to ongoing changes in land ice; such a pattern should be regarded as qualitative only in view of uncertainties in GIA models.

Figure 7(a) demonstrates that, in this particular case of the RCP4.5 scenario, the largest allowances apply to the east coast of North America and at the locations noted for Figure 7(b). Smaller values, but still at the 0.5 m level, apply to most other coasts, except for much lower values along the northern Pacific coasts of North America and northern Europe. There is general similarity of Figure 7(a) to Figure 4 of Hunter et al. (2013), although in that study allowances were considered only at the tide gauge locations themselves and the earlier A1FI emission scenario of the IPCC was employed instead of RCP4.5.

Once again, the findings in Figures 6 and 7 were found to be almost identical when using scale parameters obtained from GTSR+NEMO or GTSR+NEMO 35-day smoothed.

6. Discussion and Conclusions

A study of sea level extremes such as this has to make many assumptions. For example, there is an assumption that scale parameters derived from modelling of several decades of the present climate will be representative of those in the future. In particular, there is an assumption that the present climatology of surges remains the same. In addition, there are technical issues such as whether Gumbel distributions are adequate parameterisations of extremes calculated from tide gauge and model data (e.g. Wahl et al., 2017; IPCC, 2019, Section 4.2.3.4). As noted in Section 2, for distributions other than a Gumbel, such as the Generalised Extreme Value (GEV) or the Generalised Pareto (GPD) distributions, the slope of a plot of height against $\log(\text{ARI})$ may vary with ARI. This slope may, therefore, be regarded as a scale parameter which is 'local' to a particular ARI, with the resulting multiplication factor and allowance also varying with ARI. When a Gumbel distribution is fitted to a non-Gumbel distribution, the resultant scale parameter, multiplication factor and allowance should, therefore, be regarded as representative values for the range of ARI over which the Gumbel scale parameter is fitted. Alternatively, one might consider a completely different approach to determine scale parameters along a coastline where some tide gauge information is available, such as the Bayesian hierarchical modelling of Calafat and Marcos (2020).

The present study has focussed on the use of sea level extremes from the GTSR+NEMO model data set to determine scale parameters. In fact, we also investigated the use of alternative modelling, such as the Dynamic Atmospheric Correction (DAC) data set (Carrère and Lyard, 2003) for surges, and the Technical University of Denmark DTU-10 model for tides (Cheng and Andersen, 2010). These were found to result in an even larger under-estimate of GESLA-2 scale parameters. Nevertheless, their use was worthwhile as a partial validation of the GTSR data sets. We have not so far experimented with ocean models other than NEMO, although it should be straightforward to do so; higher resolution regional ocean models might improve the results even further. Our main conclusion from this study is that the inclusion of an ocean model such as NEMO results in the removal of most of the systematic

under-estimate of scale factors that exist using tide and surge models alone (however good they may be).

Once one has obtained reliable estimates of scale parameters for sections of coast, then it is straightforward to calculate the likely increase in the frequency of extreme levels (Equation 2) and allowances for sea level using any scenario provided by climate models (Equation 7). The second term of the allowances using GTSR+NEMO in Figure 7(b) would be approximately 30% larger, or roughly a decimetre on average, if scale factors from GTSR alone were used. That might seem a small amount in comparison to the uncertainties in predicting regional SLR itself, but it is at least a source of uncertainty that we can now account for. In addition, even small amounts such as these have major consequences with regards to the costs of future coastal protection.

There are many projections of future change in sea level available, the most recent being in the Special Report on the Ocean and Cryosphere in a Changing Climate (IPCC, 2019). However, application of the above equations to any new projection or probabilistic set of projections is a straightforward exercise (e.g. Vitousek et al., 2017; Vousdoukas et al., 2018; Taherkhani et al., 2020). For the present paper we have focused on the use of the RCP4.5 projection from the last full IPCC assessment (Church et al., 2013) which has enabled comparisons to be made to previously-reported similar findings on extreme levels. For example, the findings presented here are similar to those obtained by Hunter et al. (2013), although the present study has enabled an important extension to most of the global coastline. The new findings are also qualitatively similar to those reported in IPCC (2019, Figure 4.12) based once again on RCP4.5 projections of regional sea level change (IPCC, 2019, Figure 4.10) but using a more general parameterisation of tide gauge extremes than the Gumbel distribution used in the present paper.

In conclusion, comparison of Figure 5(a) and (b) shows that scale parameters for extreme sea levels can now be inferred with good accuracy from modelling for a large fraction of the world coastline. There remain deficiencies in both modelling and measurements. The modelling is obviously incomplete, not accounting for other coastal processes such as wave setup (Dean and Walton, 2009; Woodworth et al., 2019); we note that progress is being made on this topic (e.g. Kirezci et al., 2020). In addition, it will not account for higher-frequency local processes such as seiches that will contribute to an observed extreme sea level (Pugh et al., 2020). Surge modelling also has particular challenges in simulating the storm surges during tropical cyclones (Muis et al., 2019; Tadesse et al., 2020). Waves themselves, as opposed to still water level, also need to be taken into greater account in the study of extremes (Lambert et al., 2020). The conclusions of the latter study confirm our main finding, that omission of critical processes (waves in their case, ocean circulation in ours) tends to decrease the variance of the modelled annual maxima and the derived Gumbel scale parameters and, therefore, increase the computed multiplication factors and allowances. As regards measurements, there are still many gaps in areas such as Africa and South America where major improvements in the availability of tide gauge data are required. Such data sets are unlikely to become available for many years. Whether sea level measurements from a new generation of satellite altimetry close to the coast can provide suitable complementary information on extremes remains to be seen (Vignudelli et al., 2011). Either way, continued improvement in the combination of tide, surge and ocean modelling, properly validated by measurements, seems to offer a suitable way forward for obtaining even more reliable extreme level parameters for the global coastline.

Acknowledgements

We are grateful to Sanne Muis (Deltares) for making the GTSR model information available and for communications concerning its use. Andrew Coward and Adam Blaker (National Oceanography

Centre) are thanked for the NEMO data set. Some figures were generated using the Generic Mapping Tools (Wessel and Smith, 1998).

References

Amiruddin, A.M., Haigh, I.D., Tsimplis, M.N., Calafat, F.M., Dangendorf, S., 2015. The seasonal cycle and variability of sea level in the South China Sea. *J. Geophys. Res. Oceans* 120, 5490–5513, doi:10.1002/2015JC010923.

Bingham, R.J., Hughes, C.W. 2012. Local diagnostics to estimate density-induced sea level variations over topography and along coastlines. *J. Geophys. Res.* 117(C1), C01013, doi: 10.1029/2011JC007276.

Brodeau, L., Barnier, B., Treguier, A.M., Penduff, T., Gulev, S., 2010. An ERA40-based atmospheric forcing for global ocean circulation models. *Ocean Model.* 31, 88–104, doi:10.1016/j.ocemod.2009.10.005.

Buchanan, M.K., Kopp, R.E., Oppenheimer, M., Tebaldi, C., 2016. Allowances for evolving coastal flood risk under uncertain local sea-level rise. *Climatic Change* 137, 347-362, doi:10.1007/s10584-016-1664-7.

Calafat, F.M., Marcos, M., 2020. Probabilistic reanalysis of storm surge extremes in Europe. *P. Natl. Acad. Sci.* 117(4), 1877-1883, doi:10.1073/pnas.1913049117.

Carrère, L., Lyard, F., 2003. Modeling the barotropic response of the global ocean to atmospheric wind and pressure forcing - comparisons with observations. *Geophys. Res. Lett.* 30, 1275, doi:10.1029/2002GL016473.

Carrère, L., Lyard, F., Cancet, M., Guillot, A., Roblou, L., 2012. FES 2012: A new global tidal model taking advantage of nearly 20 years of altimetry. In 20 Years of Progress in Radar Altimetry. Venice, Italy. European Space Agency.

Cheng, Y., Andersen, O.B., 2010. Improvement in global ocean tide model in shallow water regions. Poster, SV.1-68 45, Ocean Surface Topography Science Team Meeting, Lisbon, Oct. 18-22.
https://www.space.dtu.dk/english/research/scientific_data_and_models/global_ocean_tide_model.

Church, J.A., Clark, P.U. Cazenave, A., Gregory, J.M., Jevrejeva, S., Levermann, A., Merrifield, M.A., Milne, G.A., Nerem, R.S., Nunn, P.D., Payne, A.J., Pfeffer, W.T., Stammer, D., Unnikrishnan, A.S., 2013. Sea Level Change. In: Stocker, T.F., D. Qin, G.-K. Plattner, M. Tignor, S.K. Allen, J. Boschung, A. Nauels, Y. Xia, V. Bex and P.M. Midgley (eds.), Climate Change 2013: The Physical Science Basis. Contribution of Working Group I to the Fifth Assessment Report of the Intergovernmental Panel on Climate Change. Cambridge University Press, Cambridge, United Kingdom and New York, NY, USA.

Coles, S., 2001. An Introduction to Statistical Modeling of Extreme Values. Springer, London. 208 pp.

Dean, R.G., Walton, T.L., 2009. Wave setup. Chapter 1 (pp.1-23) in, Handbook of Coastal and Ocean Engineering (ed. Y. Kim). Los Angeles: World Scientific Publishing Co. Ltd.
<http://www.worldscibooks.com/engineering/6914.html>.

Dussin, R., Barnier, B., Brodeau, L., 2014. The making of Drakkar Forcing Set DFS5. DRAKKAR/MyOcean Rep. 05-10-14, LGGE, Grenoble, France.

GTSR, 2019. Datasets of dissertation Sanne Muis. 4TU.Centre for Research Data.
<https://data.4tu.nl/repository/uuid:b6dd86f4-b182-4ad8-9bbd-e757bb8bd3c0>

Gumbel, E.J., 1941. The return period of flood flows. *Ann. Math. Stat.* 12(2), 163-190, doi:10.1214/aoms/1177731747.

Haigh, I.D., Eliot, M., Pattiaratchi, C., 2011. Global influences of the 18.61 year nodal cycle and 8.85 year cycle of lunar perigee on high tidal levels. *J. Geophys. Res.* 116, C06025, doi:10.1029/2010JC006645.

Hughes, C.W., Williams, J., Blaker, A., Coward, A., Stepanov, V., 2018. A window on the deep ocean: The special value of ocean bottom pressure for monitoring the largescale, deep-ocean circulation. *Prog. Oceanogr.* 161, 19–46, doi:10.1016/j.pocean.2018.01.011.

Hunter, J., 2012. A simple technique for estimating an allowance for uncertain sea-level rise. *Climatic Change* 113, 239-252, doi:10.1007/s10584-011-0332-1.

Hunter, J.R., Church, J.A., White, N.J., Zhang, X., 2013. Towards a global regionally varying allowance for sea-level rise. *Ocean Eng.* 71, 17-27, doi:10.1016/j.oceaneng.2012.12.041.

Hunter, J.R., Woodworth, P.L., Wahl, T., Nicolls, R.J., 2017. Using global tide gauge data to validate and improve the representation of extreme sea levels in flood impact studies. *Global Planet. Change* 156, 34-45, doi:10.1016/j.gloplacha.2017.06.007.

ICDC, 2020. Integrated Climate Data Centre. <http://icdc.cen.uni-hamburg.de/1/daten/ocean/ar5-slr.html>. Last accessed February 2020.

IPCC, 2019. IPCC Special Report on the Ocean and Cryosphere in a Changing Climate [H.-O. Pörtner, D.C. Roberts, V. Masson-Delmotte, P. Zhai, M. Tignor, E. Poloczanska, K. Mintenbeck, A. Alegría, M. Nicolai, A. Okem, J. Petzold, B. Rama, N.M. Weyer (eds.)]. In press.

Kirezci, E., Young, I.R., Ranasinghe, R., Muis, S., Nicholls, R.J., Lincke, D., Hinkel, J. 2020. Projections of global-scale extreme sea levels and resulting episodic coastal flooding over the 21st century. *Sci. Rep.* 10, 11629, doi:10.1038/s41598-020-67736-6.

Lambert, E., Rohmer, J., Le Cozannet, G., van de Wal, R.S.W., 2020. Adaptation time to magnified flood hazards underestimated when derived from tide gauge records. *Env. Res. Lett.* 15, 074015, doi:10.1088/1748-9326/ab8336.

Marcos, M., Woodworth, P.L., 2017. Spatio-temporal changes in extreme sea levels along the coasts of the North Atlantic and the Gulf of Mexico. *J. Geophys. Res. Oceans* 122, 7031-7048, doi:10.1002/2017JC013065.

McInnes, K.L., Church, J., Monselesan, D., Hunter, J.R., O'Grady, J.G., Haigh, I.D., Zhang, X., 2015. Information for Australian impact and adaptation planning in response to sea-level rise. *Australian Meteorological and Oceanographic Journal* 65, 127–149.

Menéndez, M., Woodworth, P.L., 2010. Changes in extreme high water levels based on a quasi-global tide-gauge dataset. *J. Geophys. Res.* 115, C10011, doi:10.1029/2009JC005997.

Merrifield, M.A., Genz, A.S., Kontoes, C.P., Marra, J.J., 2013. Annual maximum water levels from tide gauges: Contributing factors and geographic patterns. *J. Geophys. Res.* 118, 2535–2546, doi:10.1002/jgrc.2017.

Moat, B.I., Josey, S.A., Sinha, B., Blaker, A.T., Smeed, D.A., McCarthy, G.D., Johns, W.E., Hirschi, J.J.-M., Frajka-Williams, E., Rayner, D., Duchez, A., Coward, A.C., 2016. Major variations in subtropical North Atlantic heat transport at short (5 day) timescales and their causes. *J. Geophys. Res. Oceans* 121, 3237–3249, doi:10.1002/2016JC011660.

Muis, S., Verlaan, M., Winsemius, H.C., Aerts, J.C.J.H., Ward, P.J., 2016. A global reanalysis of storm surges and extreme sea levels. *Nat. Commun.* 7:11969, doi:10.1038/ncomms11969.

Muis, S., Verlaan, M., Nicholls, R.J., Brown, S., Hinkel, J., Lincke, D., Vafeidis, A.T., Scussolini, P., Winsemius, H.C., Ward, P.J., 2017. A comparison of two global datasets of extreme sea levels and resulting flood exposure. *Earth's Future* 5, 379-392, doi:10.1002/2016EF000430.

Muis, S., Haigh, I.D., Nobre, G.G., Aerts, J.C.J.H., Ward, P.J., 2018. Influence of El Niño-Southern Oscillation on global coastal flooding. *Earth's Future* 6, 1311-1322, doi:10.1029/2018EF000909.

Muis, S., Lin, N., Verlaan, M., Winsemius, H.C., Ward, P.J., Aerts, J.C.J.H., 2019. Spatiotemporal patterns of extreme sea levels along the western North-Atlantic coasts. *Sci. Rep.* 9, 3391, doi:10.1038/s41598-019-40157-w.

Muis, S., Irazoqui Apecechea, M., Dullaart, J., de Lima Rego, J., Madsen, K.S., Su, J., Yan, K., Verlaan, M., 2020. A high-resolution global dataset of extreme sea levels, tides, and storm surges, including future projections. *Front. Mar. Sci.* 7, 263. doi: 10.3389/fmars.2020.00263. (Gumbel scale parameters from this data set are available via doi:10.5281/zenodo.3660927.)

Pugh, D.T., Woodworth, P.L., Wijeratne, E.M.S., 2020. Seiches around the Shetland Islands. *Pure Appl. Geophys.* 177, 591-620, doi:10.1007/s00024-019-02407-w.

Slangen, A.B.A., van de Wal, R.S.W., Reerink, T.J., de Winter, R.C., Hunter, J.R., Woodworth, P.L., Edwards, T., 2017. The impact of uncertainties in ice sheet dynamics on sea-level allowances at tide gauge locations. *J. Mar. Sci. Eng.* 5, 21; doi:10.3390/jmse5020021.

Stepanov, V., Hughes, C.W., 2004. Parameterization of ocean self-attraction and loading in numerical models of the ocean circulation. *J. Geophys. Res. Oceans* 109, C03037, doi:10.1029/2003JC002034.

Tadesse, M., Wahl, T., Cid, A., 2020. Data-driven modelling of global storm surges. *Front. Mar. Sci.* 7, 260, doi:10.3389/fmars.2020.00260.

Taherkhani, M., Vitousek, S., Barnard, P.L., Frazer, N., Anderson, T.R., Fletcher, C.H., 2020. Sea-level rise exponentially increases coastal flood frequency. *Sci. Rep.* 10, 6466, doi:10.1038/s41598-020-62188-4.

van den Brink, H.W., Können, G.P., 2011. Estimating 10000-year return values from short time series. *Int. J. Climatol.*, 31, 115-126, doi:10.1002/joc.2047.

Vignudelli, S., Kostianoy, A., Cipollini, P., Benveniste, J. (eds), 2011. *Coastal altimetry*. Berlin: Springer Publishing. 578pp.

Vitousek, S., Barnard, P.L., Fletcher, C.H., Frazer, N., Erikson, L., Storlazzi, C.D., 2017. Doubling of coastal flooding frequency within decades due to sea-level rise. *Sci. Rep.* 7, 1399. doi:10.1038/s41598-017-01362-7.

Vousdoukas, M.I., Mentaschi, L., Voukouvalas, E., Verlaan, M., Jevrejeva, S., Jackson, L.P., Feyen, L., 2018. Global probabilistic projections of extreme sea levels show intensification of coastal flood hazard. *Nat. Commun.* 9, 2360, doi:10.1038/s41467-018-04692-w.

Wahl, T., Haigh, I.D., Nicholls, R.J., Arns, A., Dangendorf, S., Hinkel, J., Slangen, A.B.A., 2017. Understanding extreme sea levels for broad-scale coastal impact and adaptation analysis. *Nat. Commun.* 8, 16075, doi:10.1038/ncomms16075.

Wessel, P., Smith, W.H.F., 1998. New, improved version of generic mapping tools released. *EOS Transactions of the American Geophysical Union* 79:579-579.

Woodworth, P.L., Hunter, J.R., Marcos, M., Caldwell, P., Menéndez, M., Haigh, I., 2017. Towards a global higher-frequency sea level data set. *Geosci. Data J.* 3, 50-59, doi:10.1002/gdj3.42.

Woodworth, P.L., Melet, A., Marcos, M., Ray, R.D., Wöppelmann, G., Sasaki, Y.N., Cirano, M., Hibbert, A., Huthnance, J.M., Montserrat, S., Merrifield, M.A., 2019. Forcing factors affecting sea level changes at the coast. *Surv. Geophys.*, 40, 1351-1397, doi:10.1007/s10712-019-09531-1.

Yousef, O.M., Al-Subh, S.A., 2014. Estimation of Gumbel parameters under ranked set sampling. *J. Mod. Appl. Stat. Methods* 13, 432-443, doi:10.22237/jmasm/1414815780.

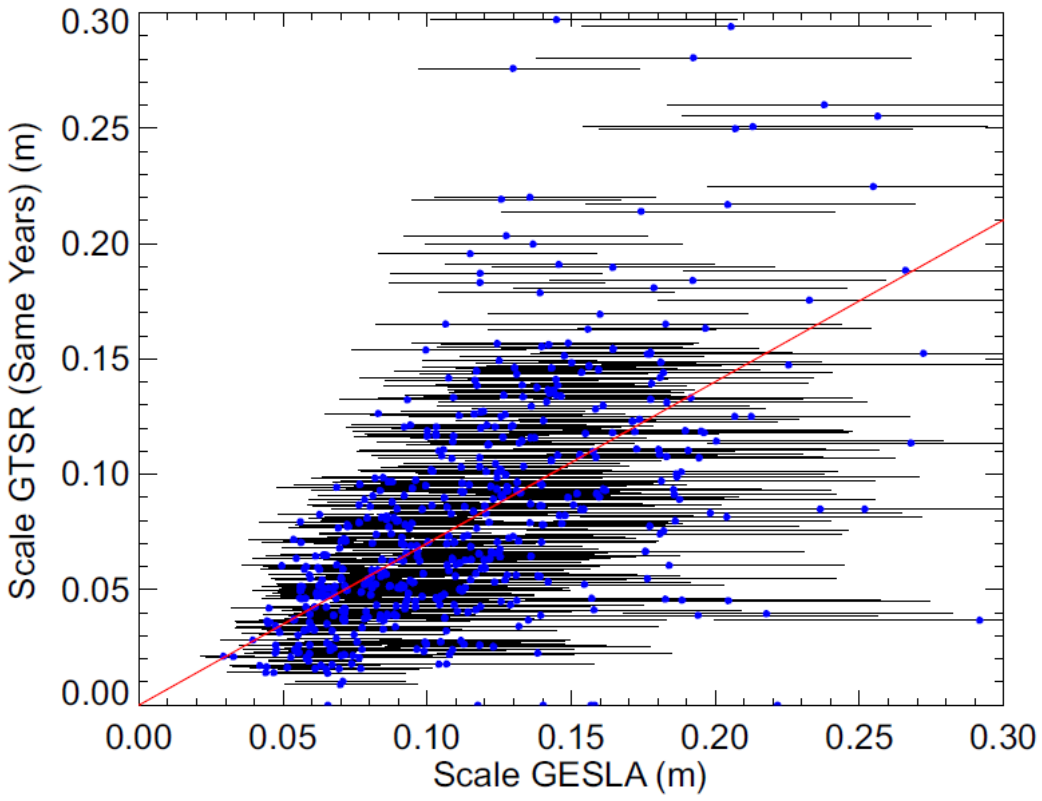
Zhai, L., Greenan, B.J.W., Hunter, J., James, T.S., Han, G., MacAulay, P., Henton, J.A., 2015. Estimating sea-level allowances for Atlantic Canada using the Fifth Assessment Report of the IPCC. *Atmos. Ocean* 53:5, 476-490, doi:10.1080/07055900.2015.1106401.

Figure captions

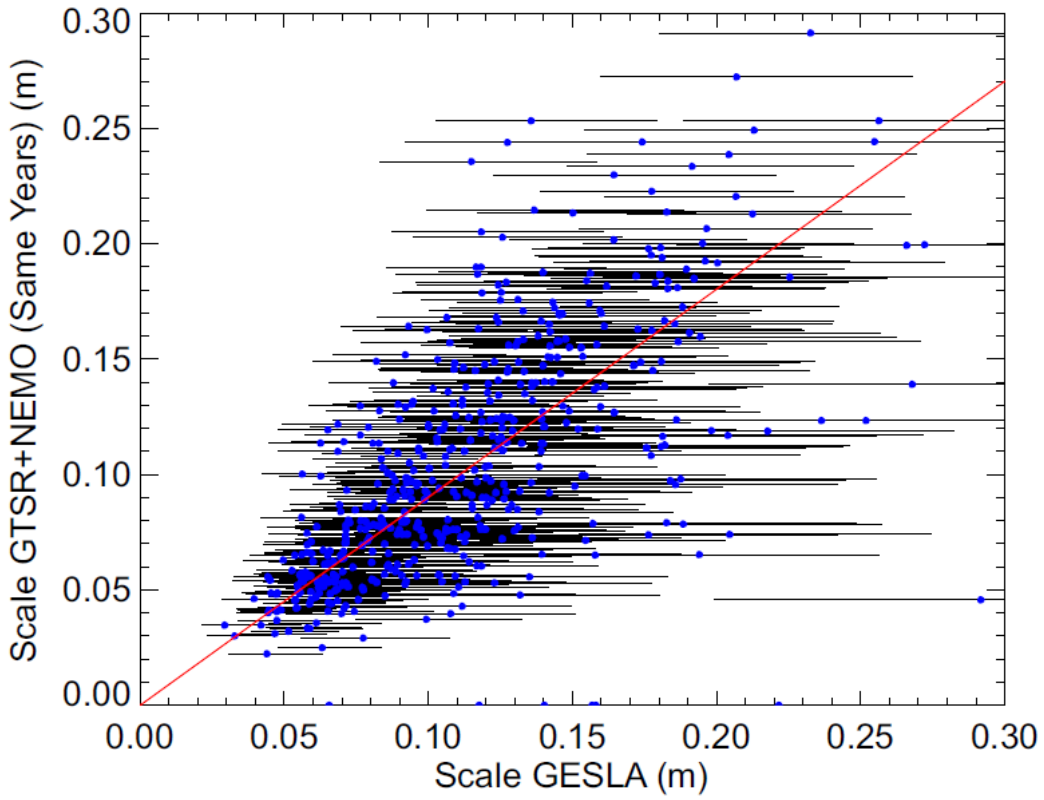
1. (a) Scale parameters from GTSR versus those derived from tide gauge records from GESLA-2 with at least 20 years of data during 1979-2012, using exactly the same years to compute the parameters. (b) Scale parameters from GTSR+NEMO versus those from GESLA-2, similarly computed. The horizontal error bars represent 95-percent uncertainty in the GESLA-2 scale parameters. The red lines are unweighted linear least-squares fits constrained to pass through the origin with the GESLA-2 value as the independent variable with slopes of 0.70 and 0.90 in (a) and (b) respectively.
2. (a) Correlation coefficients between annual maxima from GTSR and GESLA-2 with at least 20 years in common during 1979-2012 (blue), from GTSR+NEMO and GESLA-2 (red) and from GTSR+NEMO and GESLA-2 with NEMO 5-day means smoothed into 35-day means (green). (b) Distribution of coefficients using GTSR+NEMO, and (c) of the improvement in correlation using GTSR+NEMO over that using GTSR alone.
3. Scale parameters from (a) GTSR and (b) CoDEC-ERA5 versus those from GESLA-2. The modelled scale parameters were calculated using their entire data sets (1979-2014 and 1979-2017 respectively). The latter are those archived by Muis et al. (2020). The GESLA-2 scale parameters were computed from all records containing at least 20 years of data (i.e. without the restriction of 1979-onwards) with horizontal error bars representing their 95-percent uncertainties. The red lines are unweighted linear least-squares fits constrained to pass through the origin with the GESLA-2 value as the independent variable with slopes of 0.72 and 0.73 in (a) and (b) respectively.
4. Tests of combining Gumbel scale parameters. (a) Scale parameters for all 16611 GTSR coastal locations estimated using the quadratic addition of those of GTSR alone and NEMO alone (Equation 5) (y-axis) compared to those obtained from GTSR+NEMO (x-axis). The red line simply represents a ratio of 1. (b) Scale parameters estimated from the quadratic combination

of CoDEC-ERA5 and NEMO alone (Equation 6) versus those from GESLA-2 using records containing at least 20 years of data within 1979-2012 with horizontal error bars representing their 95-percent uncertainties. The red line is an unweighted linear least-squares fit constrained to pass through the origin with the GESLA-2 value as the independent variable with a slope of 0.85.

5. Reciprocal (m^{-1}) of the Gumbel scale parameter obtained from (a) tide gauge records in GESLA-2 with at least 20 years of data, and (b) estimated from GTSR+NEMO modelling.
6. The likely increase in the frequency of occurrence of extreme sea levels (the 'multiplication factor') (a) due to a spatially independent rise of 0.5 m in mean sea level, and (b) due to a spatially dependent rise provided by the RCP4.5 scenario (Church et al., 2013), using scale parameters from GTSR+NEMO.
7. (a) The overall allowance for sea level rise suggested by the RCP4.5 scenario (Church et al., 2013) together with a contribution to the allowance due to the uncertainty in the rise, and (b) the contribution to the overall allowance due to the uncertainty in the rise, using scale parameters from GTSR+NEMO. Units are metres. (c) The ratio of the contribution to the allowance due to uncertainty in the rise compared to the overall allowance itself (i.e. figures b/a). Note the colour scale saturates at 0.4 to aid visualisation of the areas where the ratio is smaller than that value.

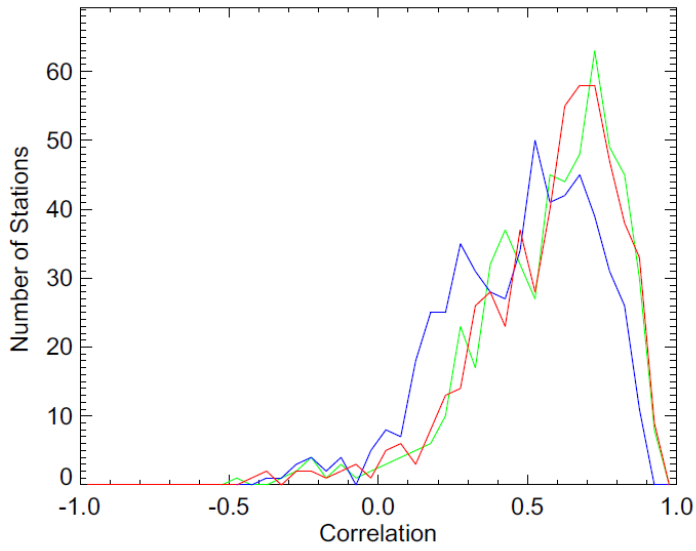


(a)

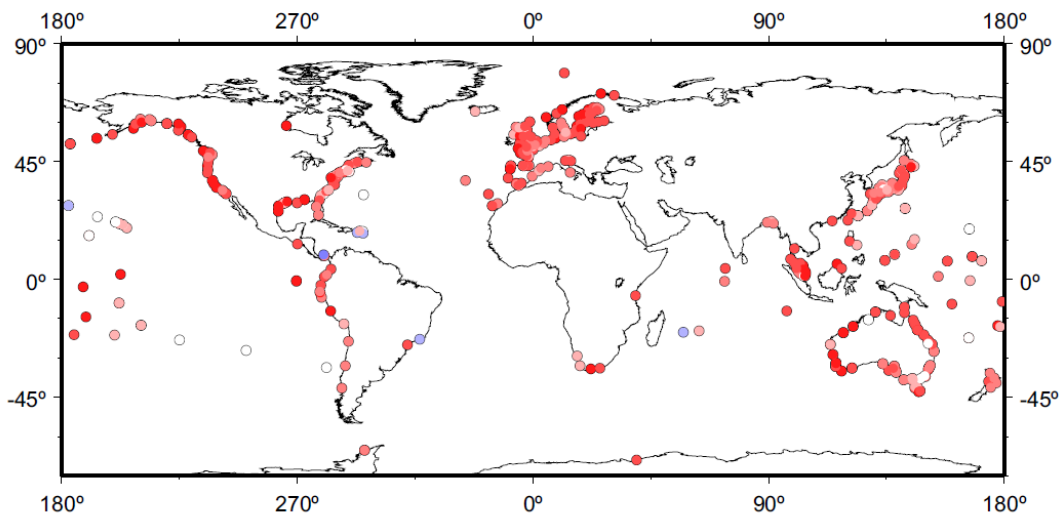


(b)

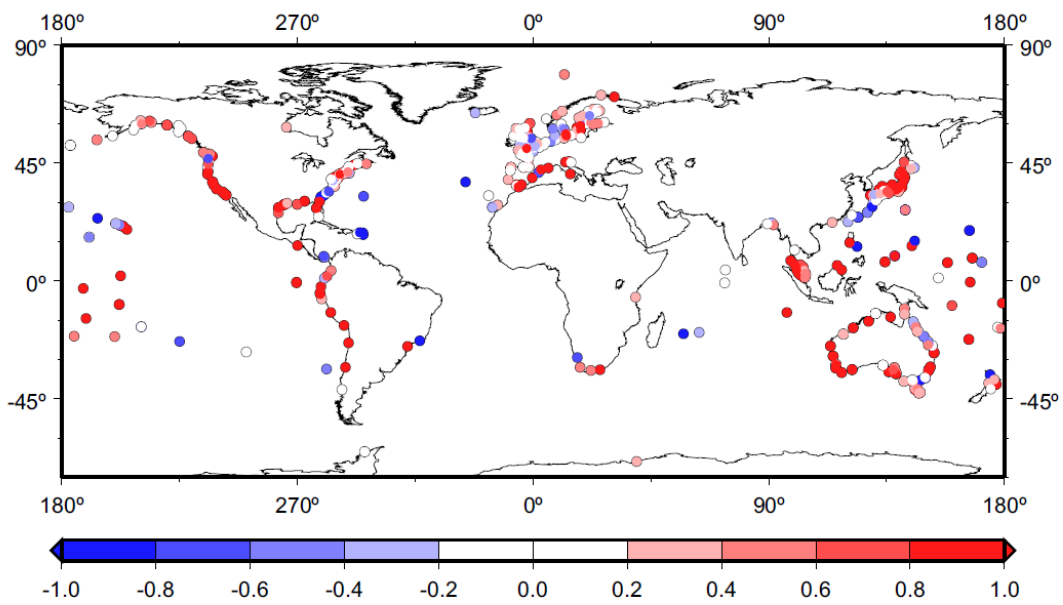
Figure 1



(a)



(b)



(c)

Figure 2

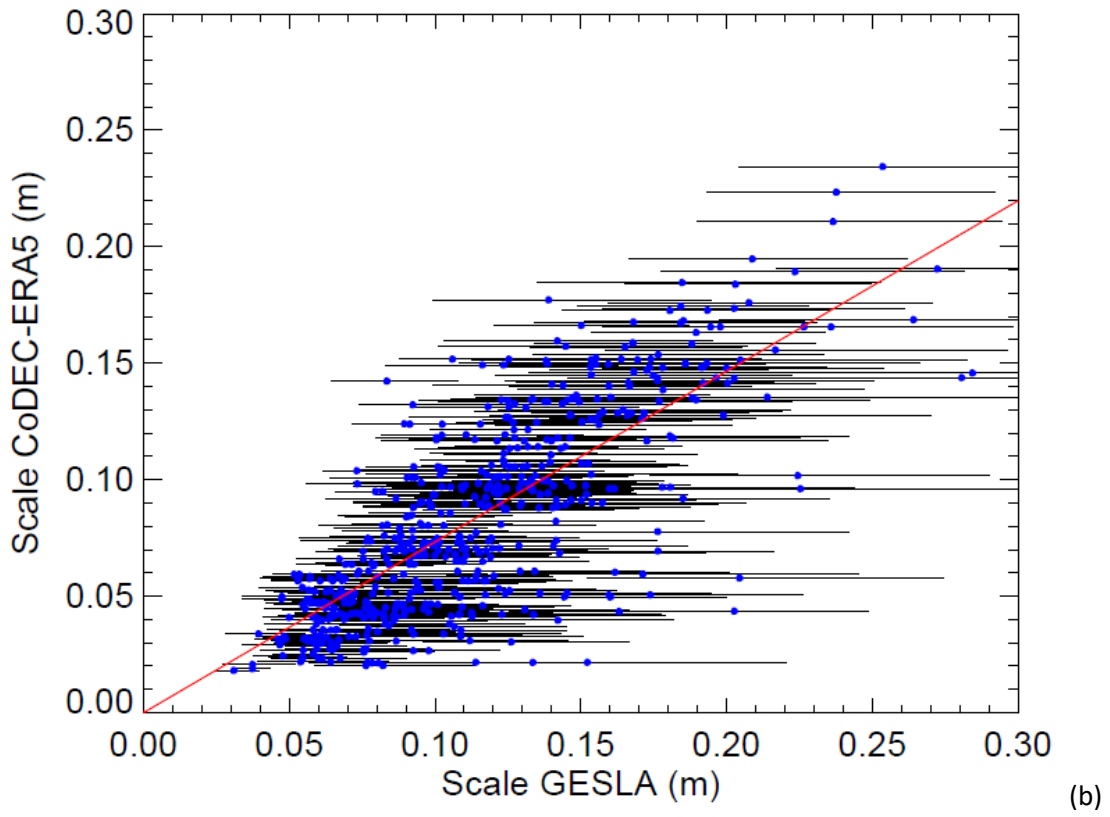
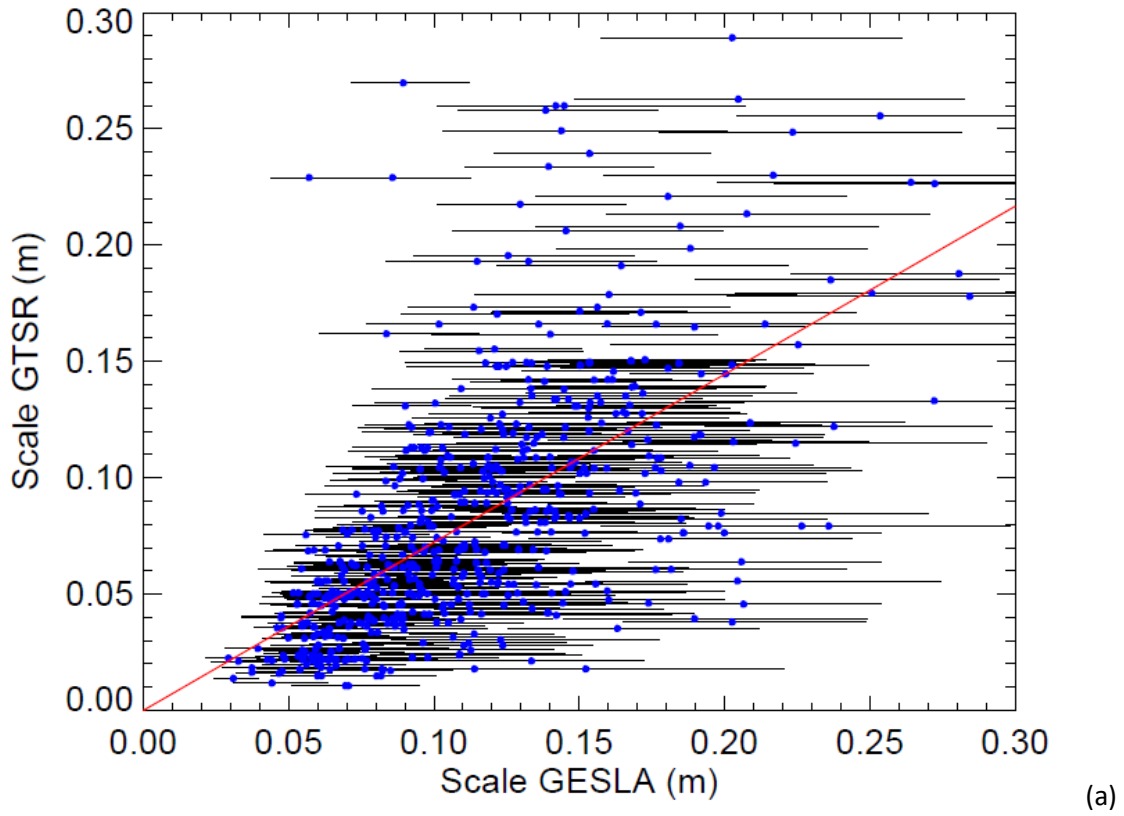
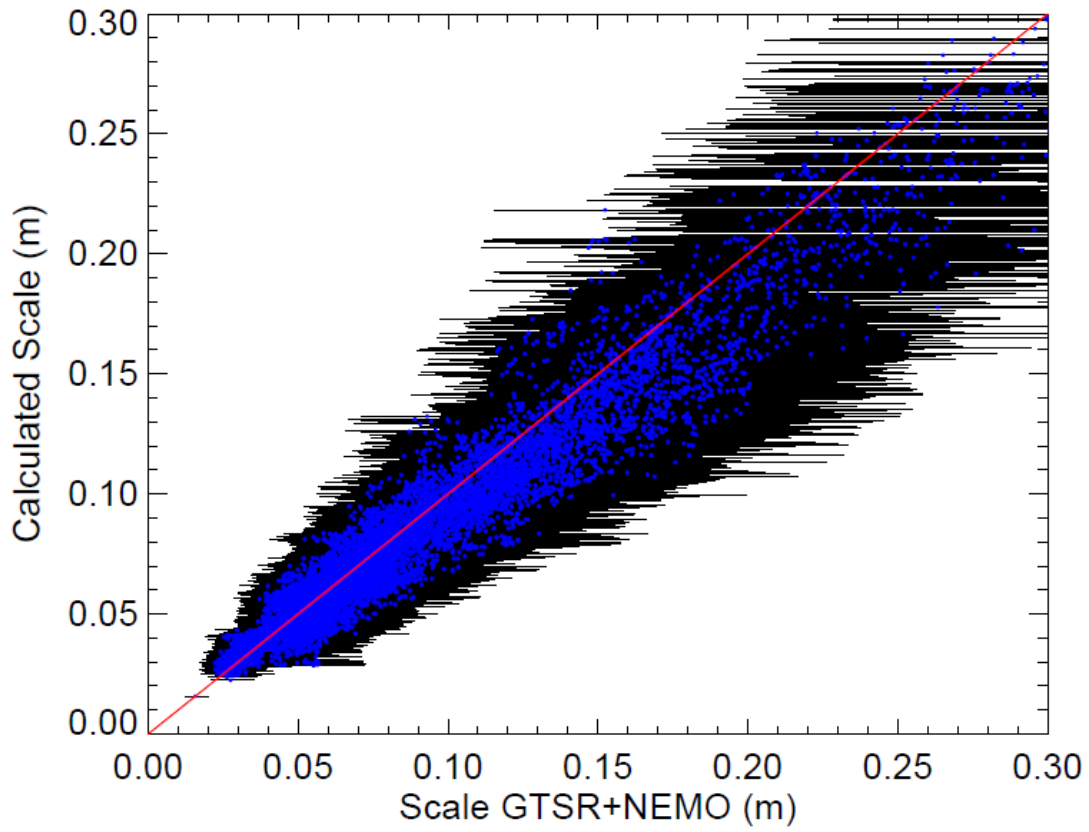
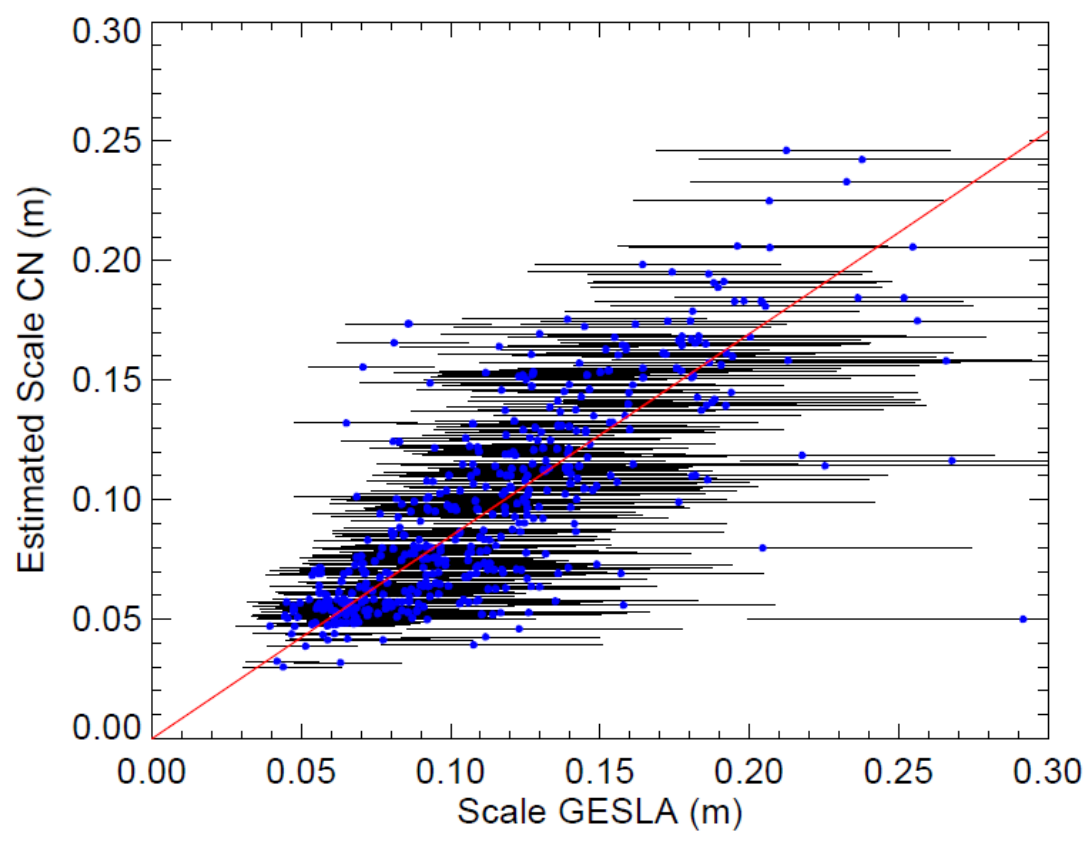


Figure 3



(a)



(b)

Figure 4

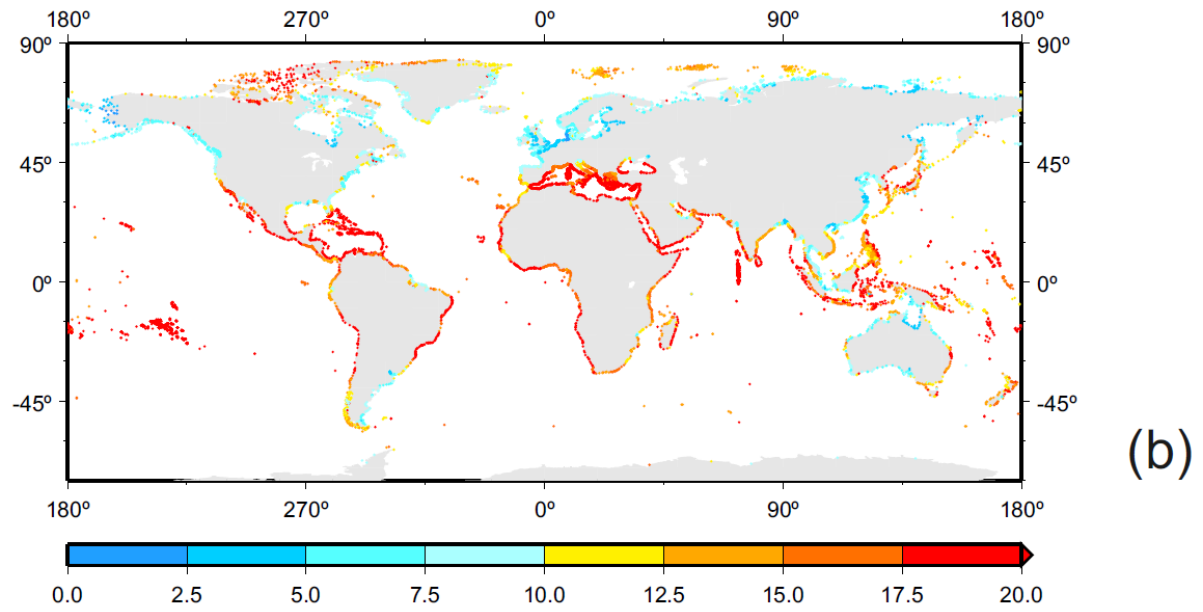
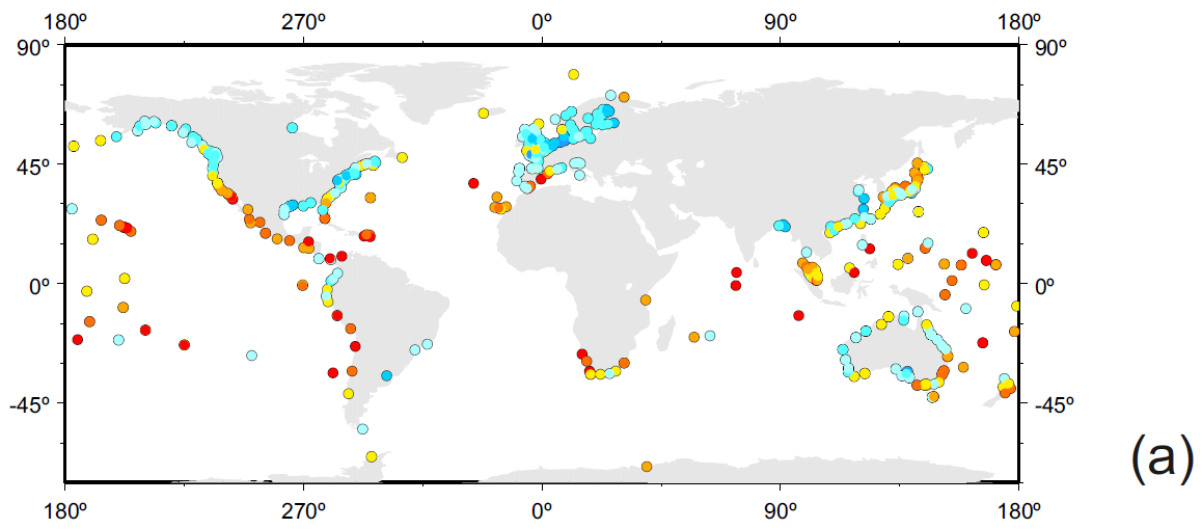


Figure 5

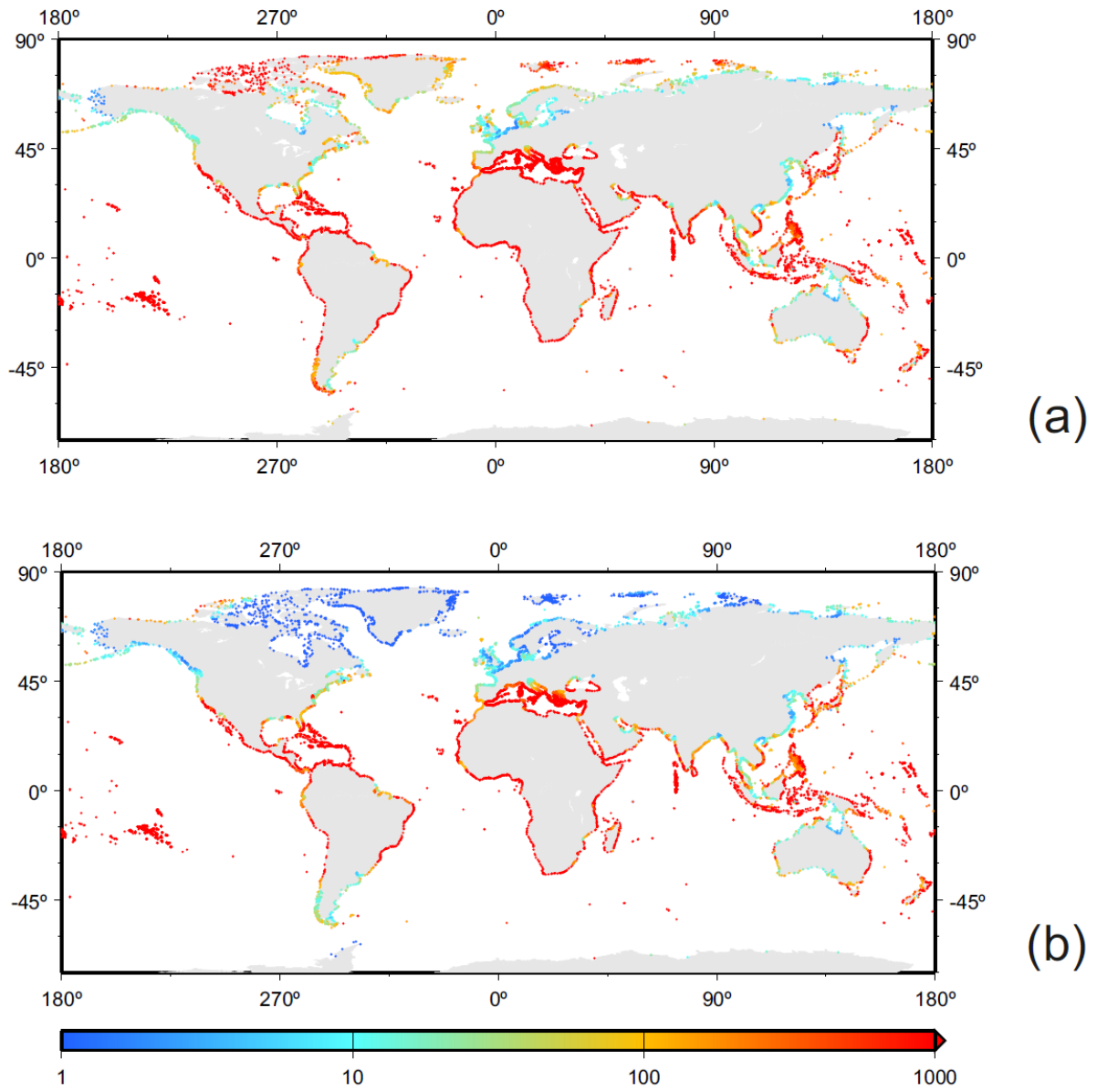
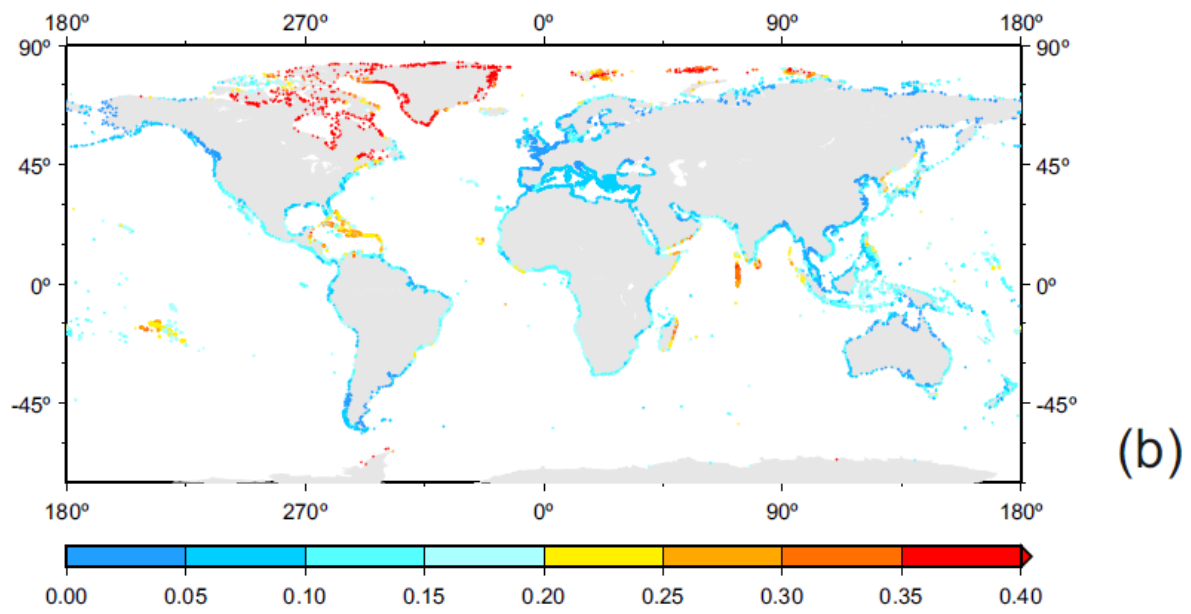
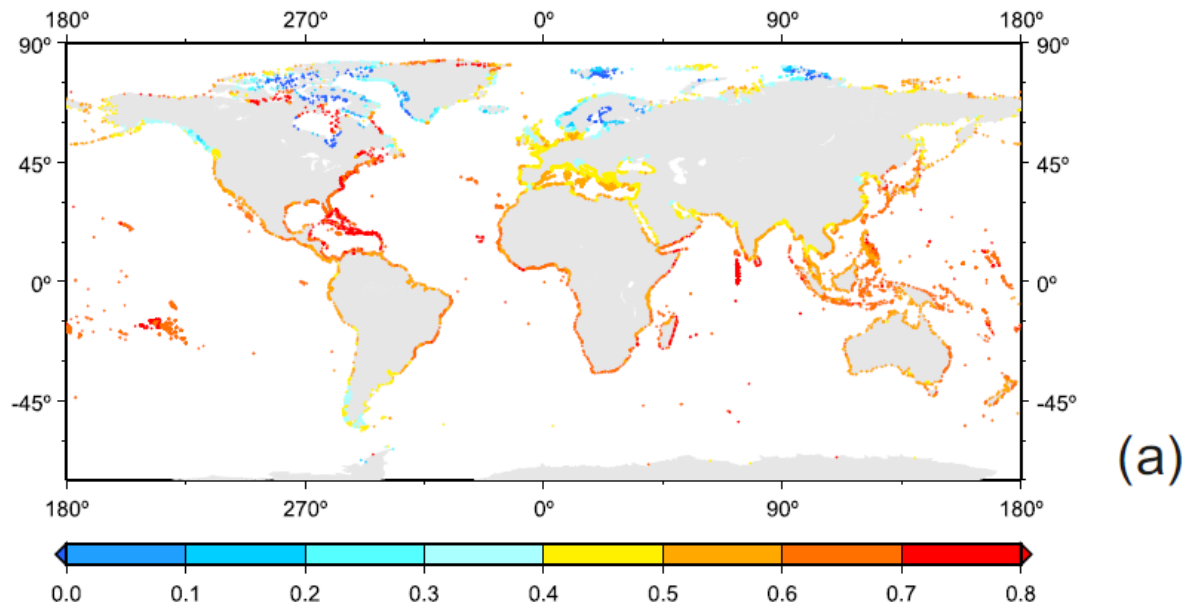


Figure 6



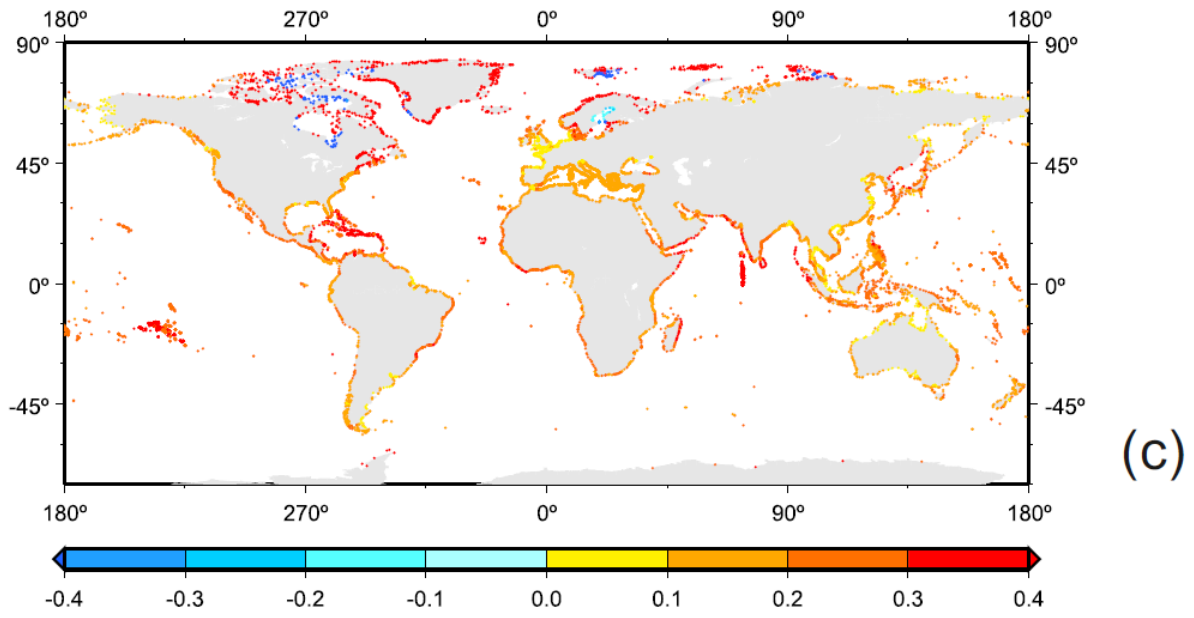


Figure 7